J. Phys.: Condens. Matter 7 (1995) L245–L251. Printed in the UK

LETTER TO THE EDITOR

# Magnetic correlations and spin dynamics in the $t$–$t'$–$J$ model

M Deeg, H Fehske and H Büttner

Physikalisches Institut, Universität Bayreuth, D-95440 Bayreuth, Germany

Received 28 February 1995

**Abstract.** Using a generalized RPA expression for the spin susceptibility, we investigate the spin dynamical properties in the normal state of the metallic cuprates on the basis of a spin-rotation-invariant slave boson representation of the $t$–$t'$–$J$ model, where the second-neighbour hopping $t'$ incorporates important correlation and band structure effects near half-filling. We attribute the contrasting $q$ dependence of the magnetic structure factor $S(q, \omega)$ seen in neutron scattering experiments for LSCO- and YBCO-type systems to differences in their Fermiology. Assuming that the antiferromagnetic correlations are spatially filtered by the hyperfine form factors, we calculate the temperature dependences of spin–lattice and spin–spin relaxation rates for planar copper and oxygen sites: the results agree qualitatively well with various experiments on $YBa_2Cu_3O_{6+x}$.

The low-energy physics of the high-$T_c$ cuprates is determined by the charge and spin dynamics in the $CuO_2$ layers. In particular, the nature of spin excitations has been extensively studied by means of nuclear magnetic/quadrupole resonance (NMR/NQR) and inelastic neutron scattering (INS) techniques clarifying the persistence of strong antiferromagnetic (AF) correlations in the normal and superconducting states [1, 2]. Detailed investigations of the wavevector dependence of the low-frequency spin fluctuation spectrum have revealed remarkable differences between the $YBa_2Cu_3O_{6+x}$ (YBCO) and $La_{2-x}Sr_xCuO_4$ (LSCO) families at low doping level $x$; the dynamic structure factor $S(q, \omega)$ keeps its maximum at $(\pi, \pi)$ in the YBCO system, while in LSCO, the peaks are displaced from the commensurate position to the four incommensurate wave vectors $(\pi \pm q_0, \pi)$, $(\pi, \pi \pm q_0)$, where $q_0 \sim 2\pi x$. On the other hand, the analysis of the NMR data shows that the relaxation rates on the planar Cu sites are similar in all materials. Two striking features are associated with $^{63}T_1^{-1}$: (i) as a result of strong local spin fluctuations on $^{63}Cu$ sites, it is enhanced by an order of magnitude over the oxygen rate $^{17}T_1^{-1}$; and (ii) in sharp contrast to the Korringa-like behaviour at the planar $^{17}O$ sites, its temperature dependence does not follow the Korringa law. Several scenarios have been proposed to analyse theoretically the neutron and nuclear relaxation data in the cuprates ranging from weak- [3, 4] and strong-coupling [5] Fermi-liquid based, phenomenological nearly AF [6, 7] and marginal Fermi-liquid schemes [8] to mean-field gauge theory approaches to the $t$–$J$ model [9].

In the present letter, we try to understand the INS and NMR experiments on the basis of a slave boson mean field theory of the $t$–$t'$–$J$ model using simple approximations for the spin susceptibility and various $q$-dependent hyperfine form factors.

The Hamiltonian describing the $t$–$t'$–$J$ model is

$$\mathcal{H}_{t-t'-J} = -t \sum_{\langle i,j\rangle,\sigma} \tilde{c}^{\dagger}_{i\sigma}\tilde{c}_{j\sigma} - t' \sum_{\langle\langle i,j\rangle\rangle,\sigma} \tilde{c}^{\dagger}_{i\sigma}\tilde{c}_{j\sigma} + J \sum_{\langle ij\rangle} \left( \boldsymbol{S}_i \cdot \boldsymbol{S}_j - \frac{n_i n_j}{4} \right). \quad (1)$$

0953-8984/95/170245+07$19.50 

The effective one-band model (1) incorporates both strong correlation and band structure effects. Apart from the usual nearest-neighbour (NN) transfer $t$, $\mathcal{H}_{t-t'-J}$ includes direct next-NN hopping processes $t'$ on a square lattice. From band structure theory, a ratio $t'/t = -0.4$ (0 to $-0.16$) has been found for the YBCO (LSCO) family, where $t = 0.3$–$0.4$ eV. Note that the $t'$ term suffices to reproduce the different Fermi surface geometries of YBCO and LSCO. Moreover, the inclusion of $t'$ coupling the same sublattice becomes crucial for the low-lying magnetic excitations. In (1), $J$ measures the AF exchange interaction.

To treat the strong electronic correlations, we adopt the $SU(2) \otimes U(1)$ spin-rotation-invariant slave boson (SRI SB) technique [10], which differs from the spinon–holon schemes [9, 11], for the $t$–$t'$–$J$ Hamiltonian. Within an SB functional integral representation of (1), the electronic operators acting in a projected Hilbert space without double occupancy are mapped onto the products

$$\tilde{c}_{i\sigma} \rightarrow \sum_{\rho} z_{i\sigma\rho} f_{i\rho} \tag{2}$$

of a fermion (anticommuting) $f_{i\rho}$ and a boson (commuting) $\mathbf{z}_i$ field operators. The hopping operators $\mathbf{z}_i^{(\dagger)} = \mathbf{z}_i^{(\dagger)}(e_i, e_i^\dagger, \mathbf{p}_i, \mathbf{p}_i^\dagger)$ yield a correlation-induced band renormalization. Here (scalar) $e_i^{(\dagger)}$ and (matrix) $\mathbf{p}_i^{(\dagger)}$ SB operators refer to empty and single-occupied states at site $i$. The (pseudo-) fermions $f_{i\rho}^\dagger$ are components of a spinor field $\Psi_i^\dagger = (f_{i\alpha}^\dagger, f_{i\beta}^\dagger)$ and hence SRI is ensured. The interaction term is bosonized via

$$n_i \rightarrow 2 \operatorname{Tr} \mathbf{p}_i^\dagger \mathbf{p}_i \tag{3}$$

$$S_i \rightarrow \operatorname{Tr} \mathbf{p}_i^\dagger \tau \mathbf{p}_i . \tag{4}$$

Unphysical states in the extended (bosonic and fermionic) Fock space are eliminated by imposing a set of local constraints:

$$e_i^\dagger e_i + 2 \operatorname{Tr} \mathbf{p}_i^\dagger \mathbf{p}_i = 1 \qquad \text{completeness} \tag{5}$$

$$\Psi_i \otimes \Psi_i^\dagger + 2\mathbf{p}_i^\dagger \mathbf{p}_i = \tau_o \qquad \text{(1–1–correspondence).} \tag{6}$$

Using the SRI SB functional integral theory at the saddle point level, we have studied [12] the *static* magnetic properties of the 2D $t$–$t'$–$J$ model, in particular the ground-state phase diagram, including incommensurate magnetic structures and phase-separated states. Furthermore we have calculated the doping dependence of the Hall resistivity, the results being in accord with experiments on $La_{2-x}Sr_xCuO_4$, $YBa_2Cu_3O_{6+x}$ and $Nd_{2-x}Ce_xCuO_4$ [13]. In this letter, we focus on the spin *dynamical* properties in the *paraphase* of the extended $t$–$J$ model (1), where we will use an RPA-like form for the exchange-enhanced spin susceptibility [9, 11, 14]

$$\chi_s(q, \omega) = \frac{\overline{\chi}_o(q, \omega)}{1 + (J/2)(\cos q_x + \cos q_y)\overline{\chi}_o(q, \omega)} . \tag{7}$$

The irreducible susceptibility $\overline{\chi}_o(q, \mathrm{i}\omega_m) = -(2/\beta N) \sum_{k,n} \overline{G}(k, \mathrm{i}\omega_n)\overline{G}(k + q, \mathrm{i}\omega_{n+m})$ contains the (dressed) SB Green propagators $\overline{G}(k, \mathrm{i}\omega_n) = [\mathrm{i}\omega_n - E_k + \tilde{\mu}]^{-1}$ describing non-interacting electrons with a *renormalized* band structure

$$E_k = -2z^2 t \left[\cos k_x + \cos k_y + 2(t'/t) \cos k_x \cos k_y\right] . \tag{8}$$

The (shifted) chemical potential $\tilde{\mu}$ is fixed by the requirement $n = (2/N) \sum_k [\exp(\beta(E_k - \tilde{\mu})) + 1]^{-1}$, where $\beta = 1/k_B T$. Note that the band renormalization factor $z^2 = 2\delta/(1 + \delta)$ varies strongly with hole concentration $\delta = 1 - n$.

Once the dynamic spin susceptibilty has been obtained, both INS measurements and NMR/NQR experiments can be explored. From the fluctuation–dissipation theorem the $q$- and $\omega$-dependent spin structure factor

$$S(q,\omega) = \frac{1}{\pi}\frac{1}{1-\exp(-\beta\hbar\omega)}\operatorname{Im}\chi_s(q,\omega) \tag{9}$$

probed by INS is related to the dynamical susceptibility. On the other hand, the nuclear spin–lattice relaxation rate ${}^aT_{1\alpha}^{-1}$ ($\alpha = \perp, \parallel$), e.g. for a field $H_\alpha$ applied parallel to the $c$ axis, given by [6]

$$\left({}^aT_{1\parallel}T\right)^{-1} = \frac{1}{2}\frac{k_B}{\mu_B^2\hbar}\lim_{\omega\to 0}\frac{1}{N}\sum_q^a F_\perp^2(q)\frac{\operatorname{Im}\chi_s(q,\omega)}{\hbar\omega} \tag{10}$$

and transverse spin–spin relaxation rate, $T_{2G}^{-1}$, for the RKKY coupling of the nuclear Cu spins given by [15]

$$T_{2G}^{-2} = \frac{c}{8\hbar^2}\frac{1}{(2\mu_B)^4}\left\{\frac{1}{N}\sum_q\left(F_\parallel^2(q)\chi_s(q)\right)^2 - \left(\frac{1}{N}\sum_q F_\parallel^2(q)\chi_s(q)\right)^2\right\} \tag{11}$$

provide local, atomic-site- ($a = \{63, 17\}$-) specific information. Here $\mu_B$ denotes the Bohr magneton and the constant $c = 0.69$ is the natural abundance fraction of the $^{63}$Cu isotope. The form factors are given for $^{63}$Cu and the planar $^{17}$O nucleus as [16]

$${}^{63}F_\alpha(q) = A_\alpha + 2B(\cos q_x + \cos q_y) \tag{12}$$

$${}^{17}F_\alpha(q) = 2C\cos(q_x/2). \tag{13}$$

Together with the anisotropy of the Cu relaxation rates, the measurements of the Knight shift

$${}^aK_\alpha = \frac{1}{2}\frac{1}{\mu_B^a\gamma_n\hbar}\lim_{q\to 0}{}^aF_\alpha(q)\chi_s(q,\omega=0) \tag{14}$$

have been used to determine the hyperfine coupling constants $A_\alpha$, $B$ and $C$ on the basis of the Mila–Rice Hamiltonian [17]. Following [6] we take $A_\parallel \approx -4B$, $A_\perp \approx 0.84B$, $C \approx 0.87B$ and $B \approx 3.3\times 10^{-7}$ eV, where ${}^{63}\gamma\hbar = 7.5\times 10^{-24}$ erg G$^{-1}$ and ${}^{17}\gamma\hbar = 3.8\times 10^{-24}$ erg G$^{-1}$.

In order to make contact with the experimental situation in the cuprates, in the numerical work we fix $J/t = 0.4$, and take $t = 0.3$ eV as the energy unit. As we know, the RPA susceptibility contains an unphysical instability of the paramagnetic phase at some particular wave vector $q$ below a critical doping $\delta_c$ as signalled by the zero in the denominator of (7) at $\omega = 0$ (Stoner condition). Therefore the use of (7) only makes sense if the system is far from the magnetic instability, i.e., $\delta > \delta_c$, where for $J = 0.4$ we have $\delta_c(t'/t = -0.16) \simeq 0.27$ and $\delta_c(-0.4) \simeq \delta_c(0) \simeq 0.17$.

We begin with a discussion of the RPA dynamical spin structure factor $S(q,\omega)$. The $q$ dependence of $S(q,\omega)$ along the main symmetry axis of the Brillouin zone is shown in figure 1 for different ratios $t'/t$, $J = 0.4$ and hole density $\delta = 0.3$. Here the temperature is $T = 35$ K and the frequency $\hbar\omega = 10$ meV. For LSCO-type parameters ($t'/t = 0, -0.16$) we found four pronounced incommensurate peaks located at the points $(\pi \pm q_0, \pi)$, $(\pi, \pi \pm q_0)$. The incommensurate modulation wave vectors move with increasing doping level $\delta$ away from the corner of the Brillouin zone along the directions $(1,\pi)$ or $(\pi, 1)$ (square lattice notation). Note that while the incommensurate peak position obtained from a three-band RPA calculation of $S(q,\omega)$ [5] can be parametrized consistent with the experimental observation that $q_0 \simeq 2\pi x$ [18], all the effective one-band RPA approaches [9, 19] yield

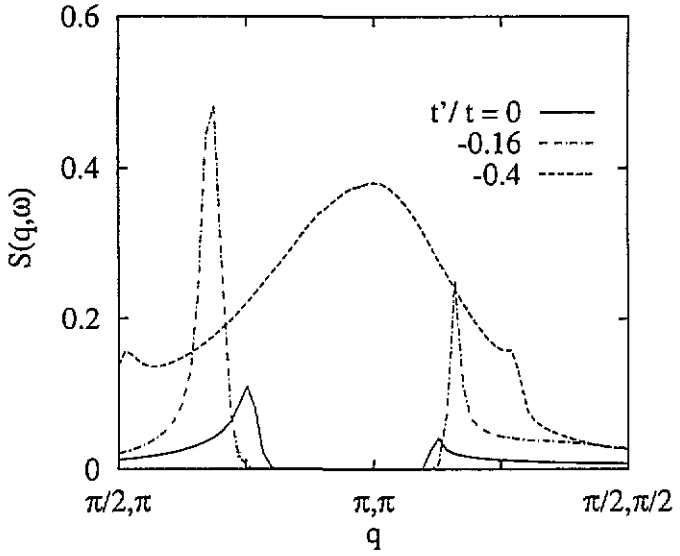


**Figure 1.** Dynamic magnetic structure factor $S(q, \omega)$ plotted along the (1,1) and $(1, \pi)$ directions of the Brillouin zone for different ratios $t'/t$.

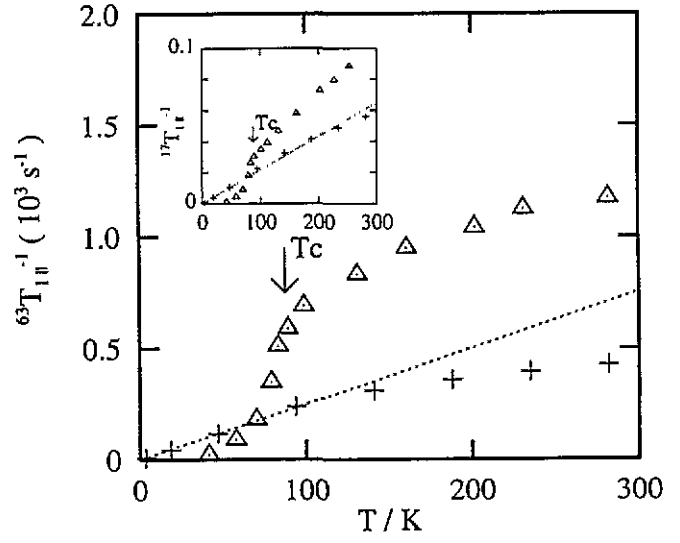


**Figure 2.** Spin–lattice relaxation rates $^{63}T_{1\parallel}^{-1}$ and $^{17}T_{1\parallel}^{-1}$ (inset) as a function of temperature. SB results (+; $t'/t = -0.4, \delta = 0.35$) are compared with experiments ($\Delta$) on $YBa_2Cu_3O_7$ [23].

an incommensurability scaling rather as $q_0 \simeq \pi\delta$ (in the LSCO systems the concentration of the chemically doped charge carriers in the $CuO_2$ planes ($\delta$) definitely agrees with the composition ($x$) of the substituent Sr). A more detailed investigation of the LSCO-type $q$ scans show that the $q$ variation of $S(q, \omega)$ is mainly governed by that of $\overline{\chi}_0(q, \omega)$ and, in accordance with experiments [20], the incommensurate peaks considerably broaden as temperature or energy transfer are increased [21]. By contrast, the same plot for YBCO-type ($t'/t = -0.4$) parameters shows a broad, nearly $T$-independent [21], maximum around the $(\pi, \pi)$ point [22] (see figure 1) which, due to the flat topology of $\overline{\chi}_0$, mainly

reflects the $q$ dependence of $J(q)$ (cf. (7)). In this way, our calculations confirm recent arguments [5, 8, 9] for the importance of band structure (Fermi-surface geometry) effects in explaining the difference between observed LSCO and YBCO spin dynamics. Nevertheless, the question whether the incommensurate signals arise from an intrinsic magnetic structure or whether they result from the formation of domains (charge superstructures) in the LSCO system remains unanswered by INS [2, 16].

In a next step, we calculate the longitudinal or spin–lattice relaxation rate, $T_1^{-1}$, using the hyperfine form factors (12) and (13). In figure 2 the temperature dependences of $^{63}T_{1\|}^{-1}$ and $^{17}T_{1\|}^{-1}$ (inset) are shown for $\delta = 0.35$ and $t'/t = -0.4$ in comparison with experiments [23] on fully oxygenated YBCO materials ($x = 1$). Although our theory does not succeed in giving the correct amplitude of $^{a}T_{1\|}^{-1}$ the qualitative features of the NMR data are described surprisingly well. Obviously the broad magnetic peak in $S(q, \omega)$ at the AF wave vector $Q_{AF} = (\pi, \pi)$ strongly enhances the relaxation rate on Cu sites while, due to a geometrical cancellation ($^{17}F_{\alpha}(q \simeq Q_{AF}) \simeq 0$), the corresponding oxygen rate is rather insensitive to nearly commensurate AF fluctuations, and therefore is governed by the long-wavelength part $q \simeq 0$ of the spin susceptibility [2]. For $^{63}$Cu, the nominal Korringa ratio $S \equiv (1/T_1 T K_S^2)$ ($K_S$ denotes the spin part of the Knight shift) is at least one order of magnitude larger. As can be seen from figure 2, for $YBa_2Cu_3O_7$-type parameters, a Korringa ($1/T_1 \propto T$) dependence (dotted line) holds at both Cu and O sites below $T^* \sim 120$ K, demonstrating the existence of a characteristic temperature $T^*$ as in all other near-optimum-$T_c$ compounds [2, 24]. $T^*$ is in good agreement with the coherence energy scale suggested experimentally [24]. Above $T^*$, the $^{17}$O NMR relaxation remains linear whereas the $^{63}$Cu relaxation time does not follow the Korringa law. Similar results are found for the LSCO system [21].

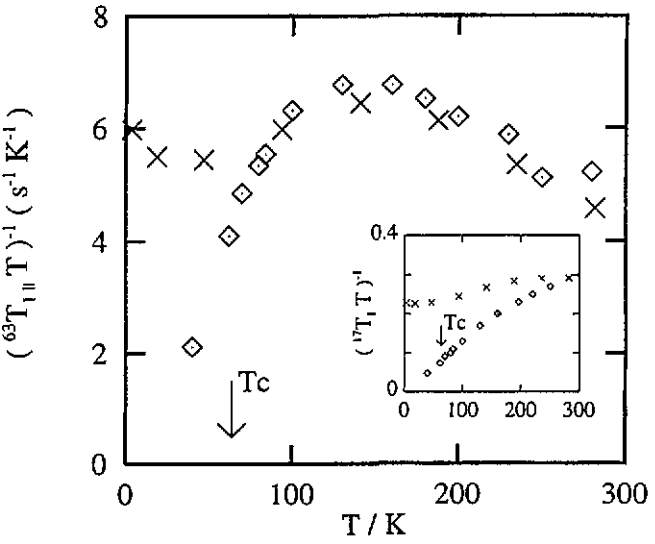


**Figure 3.** $^{63}$Cu and planar $^{17}$O relaxation data (◇) for underdoped $YBa_2Cu_3O_{6.6}$ [25] are plotted against temperature. Theoretical results (×) are given at $t'/t = -0.4$ and $\delta = 0.2$.

In the oxygen-deficient compound $YBa_2Cu_3O_{6.6}$, $1/(^{63}T_{1\|}T)$ shows a broad maximum at about 150 K (see figure 3), which reflects a strong deviation from the canonical Korringa behaviour. In the normal state regime the theoretical results agree even quantitatively with the experimental $^{63}$Cu NMR data [25]. At this point it is important to stress that the present theory incorporates considerable band renormalization effects already via $\overline{\chi}(q, \omega)$, especially

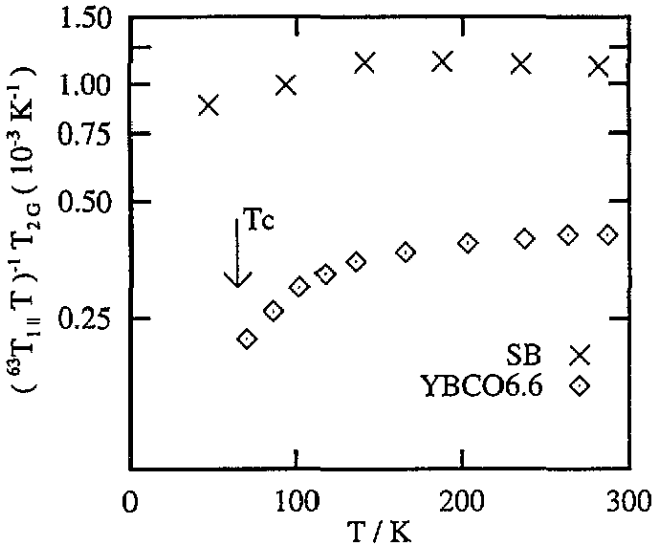


**Figure 4.** $T_{2G}/(^{63}T_{1\|}T)$ in underdoped $YBa_2Cu_3O_{6.6}$ (◇) as measured by Takigawa [15] compared with the SB data (×) at $t'/t = -0.4$ and $\delta = 0.2$.

at low doping level. Thus a rather moderate strength $J = 0.4$ of the AF exchange interaction yields the experimentally observed enhancement of $^{63}T_{1\|}^{-1}$. In striking contrast to the optimally doped YBCO system, the Korringa relation is no longer satisfied for the planar $^{17}O$ nucleus sites in the underdoped material (cf. inset figure 3). Instead, a different behaviour $^{17}T_{1\|}T^{17}K_S$ = constant was suggested to hold down to $T_c$ [25]. The unconventional $T$ scaling of $^{17}T_{1\|}$ has been taken as a signature for another important feature of the normal state spin dynamics, the so-called spin gap behaviour [2].

Complementary measurements of the transverse spin–spin relaxation rate, $T_{2G}^{-1}$, have provided further insights into the drastic change in the magnetic properties when passing from the overdoped to the underdoped regime [15, 26]. As experimentally observed, we found that $T_{2G}^{-1}$ increases (decreases) with increasing (decreasing) hole doping (temperature) [21]. In order to detect the opening of a spin pseudogap as a function of $T$, a powerful technique is to measure the ratio $T_{2G}/T_1T$ [27] which is nearly constant above ~ 200 K for deoxygenated $YBa_2Cu_3O_{6.6}$ [15]. The calculated temperature dependence of this quantity is shown in figure 4 together with recent experimental results [15]. Most noticably, the opening of a spin pseudogap at $T^* \simeq 135$ K [27], i.e. well above $T_c$, is clearly seen as a decrease of $T_{2G}/T_1T$ below $T^*$. Note that for $YBa_2Cu_3O_7$, as predicted by Fermi liquid theories, the ratio $T_{2G}^2/T_1T$ is approximately constant above ~ 150 K [2].

In conclusion, we have shown that our SB treatment of the spin dynamics in high–$T_c$ compounds, which incorporates important strong correlation and band structure (Fermi surface) effects in terms of the $t$–$t'$–$J$ model, provides a reasonable explanation of the basic features of both INS and NMR experiments on LSCO and YBCO systems.

This work was performed under the auspices of Deutsche Forschungsgemeinschaft, SFB 213 (TOPOMAK), Bayreuth. The authors would like to thank D Ihle for critical reading of the manuscript.

## References


[1] For a recent overview of the experimental situation see Wyder P (ed) 1994 *Proc. Int. Conf. $M^2S$ HTSC IV, (Grenoble) Physica* **135–240**
[2] Kampf A P, *Phys. Rev.* 1994 **249** 219
[3] Bulut N, Hone D W, Scalapino D J, and Bickers N E 1990 *Phys. Rev.* B **41** 1797
[4] Lavagna M and Stemmann G 1994 *Phys. Rev.* B **49** 4235
[5] Si Q, Zha Y, Levin K and Lu J P 1993 *Phys. Rev.* B **47** 9055
[6] Millis A J, Monien H, and Pines D 1990 *Phys. Rev.* B **42** 167
[7] Monthoux P and Pines D 1994 *Phys. Rev.* B **50** 16015
[8] Littlewood P B, Zaanen J, Aeppli G and Monien H 1993 *Phys. Rev.* B **48** 487
[9] Tanamoto T, Kohno H and Fukuyama H 1993 *J. Phys. Soc. Japan* **62** 717; 1994 **63** 2739
[10] Deeg M, Fehske H and Büttner H 1994 *Europhys. Lett.* **26** 109
[11] Grempel D R and Lavagna M 1992 *Solid State Commmun.* **83** 595
[12] Deeg M and Fehske H 1994 *Phys. Rev.* B **50** 17874
[13] Fehske H and Deeg M 1995 *Solid State Commun.* **93** 41
[14] Si Q 1994 *Int. J. Mod. Phys.* B **1 & 2** 47
[15] Takigawa M 1994 *Phys. Rev.* B **49** 4158
[16] Barzykin V, Pines D and Thelen D 1994 *Phys. Rev.* B **50** 16052
[17] Mila F and Rice T M 1989 *Physica* C **157** 561
[18] Cheong S W *et al* 1991 *Phys. Rev. Lett.* **67** 1791
[19] Bénard P, Chen L and Tremblay A-M S 1993 *Phys. Rev.* B **47** 15217
[20] Mason T E, Aeppli G and Mook H A 1992 *Phys. Rev. Lett.* **68** 1414
[21] Deeg M 1995 *Thesis* University of Bayreuth
[22] Rossat-Mignod J *et al* 1991 *Physica C* **185–189** 86
[23] Takigawa M *et al* 1989 *Physica* C **162** 853
[24] Hammel P C *et al* 1989 *Phys. Rev. Lett.* **63** 1992
[25] Takigawa M *et al* 1991 *Phys. Rev.* B **43** 247
[26] Itoh Y *et al* 1992 *J. Phys. Soc. Japan* **61** 1287
[27] Berthier C *et al* 1994 *Physica* C **235–240** 67